JOURNAL OF INDUSTRIAL AND
MANAGEMENT OPTIMIZATION
Volume **6**, Number **3**, August **2010**

doi:10.3934/jimo.2010.6.569

pp. **569–585**

EXACT PERFORMANCE ANALYSIS OF A SINGLE-WAVELENGTH OPTICAL BUFFER WITH CORRELATED INTER-ARRIVAL TIMES

Wouter Rogiest, Dieter Fiems, Koenraad Laevens and Herwig Bruneel

SMACS Research Group, Department TELIN (IR07), Ghent University
St.-Pietersnieuwstraat 41, 9000 Gent, Belgium

Abstract. Providing a photonic alternative to the current electronic switching in the backbone, optical packet switching (OPS) and optical burst switching (OBS) require optical buffering. Optical buffering exploits delays in long optical fibers; an optical buffer is implemented by routing packets through a set of fiber delay lines (FDLs). Previous studies pointed out that, in comparison with electronic buffers, optical buffering suffers from an additional performance degradation. This contribution builds on this observation by studying optical buffer performance under more general traffic assumptions. Features of the optical buffer model under consideration include a Markovian arrival process, general burst sizes and a finite set of fiber delay lines of arbitrary length. Our algorithmic approach yields instant analytic results for important performance measures such as the burst loss ratio and the mean delay.

1. **Introduction.** With the popularity of multimedia services and e-commerce applications boosting the hunger for Internet bandwidth, adding capacity to the backbone is a natural and necessary concern. Currently, IP packets travel from hop to hop over optical fiber and are converted into electricity in order to extract header data and buffer them. Then, the packets are converted back into light and are transmitted to the next hop. This conversion to electricity is expected to be a bottleneck in terms of conversion speed in the near future. Hence, research is directed to packet or (at least) payload forwarding without conversion.

For both optical packet switching (OPS) [6] and optical burst switching (OBS) [14, 5] solutions, nodes have to handle contention that arises whenever two or more packets or bursts simultaneously head for the same destination. In general, a combination of wavelength conversion and buffering offers the most viable solution to date. Since light cannot be frozen, optical buffering is implemented by delaying the light with a set of fiber delay lines (FDLs). Although feasible with off-the-shelf components, such an optical buffer has several drawbacks when compared to electronic memory. Size is an obvious drawback, for typical OBS specifications (a 10

2000 *Mathematics Subject Classification.* Primary: 68M20, 60K25; Secondary: 90B22.

Key words and phrases. performance evaluation, queueing theory, optical buffers, FDL buffers.
This paper was presented at the QTNA2009 conference which was held in Singapore during July 29–August 1, 2009. An earlier and brief version of this paper was published in the Conference Proceedings. The reviewing process of the paper was handled by Wuyi Yue, Yutaka Takahashi and Hideaki Takagi as Guest Editors.

The second author is a postdoctoral fellow with the Research Foundation Flanders (F.W.O.-Vlaanderen), Belgium.

Gbps link and 100 kbit burst sizes), approximately 2 km of fiber delays bursts for the duration of a single burst. Hence, the number of fibers and their lengths are limited, which results in a reduced buffer capacity in comparison with electronic buffers. A second drawback is caused by the optical buffer's implementation itself. Since the buffer can only provide a limited number of delays, it often cannot assign the exact delay needed. Typically a somewhat larger delay, equal to the length of one of the available fiber delay lines is assigned. This results in "voids" on the outgoing channel, and implies capacity loss. As a consequence, the waiting times and loss probability of optical buffers increase in comparison with their electronic counterparts.

Although Lakatos analyzed a similar system as early as 1994 [9], Callegati [2, 3, 4] was the first to analytically investigate the performance of optical buffers with variable length packets. He provides an approximating model for a single-wavelength optical buffer model with Poisson arrivals and exponentially distributed burst sizes. Extending the analysis to general burst sizes, Laevens and Bruneel [8] present a performance analysis with probability generating functions for an FDL buffer in discrete time, which yields exact results for infinite system size and approximate results for finite system size. The continuous-time counterpart of their model is investigated in [15], while the FDL buffer model with more generally distributed inter-arrival times is the subject of [10, 11, 17].

While the analyses of [8, 15, 10, 11, 17] center on the evolution of the scheduling horizon, more recent contributions capitalize on the system properties by studying the evolution of the waiting times. Due to the fact that an FDL buffer's structure inherently limits the number of possible waiting times, an analysis in terms of the waiting time allows for a simplified analysis. Exploiting this, Almeida et al. [1] obtain a Markov-chain-based solution that holds for generally distributed inter-arrival and burst sizes with low numerical complexity, which is however not exact unless one makes simplifying assumptions. Guaranteeing exact results, the assumptions are relaxed in [12, 16, 18, 19]. There, Poisson arrivals and general burst sizes [16, 19] and general uncorrelated inter-arrival times and burst sizes [18] are assumed while there are no restrictions on the lengths of the FDLs. Further, very recently, also an analysis with feedback Markov fluid flows has been proposed [7].

The current contribution builds on the approach of [12, 16, 18, 19]. The essential novelty is that we assume correlation between subsequent inter-arrival times instead of independent arrivals [12, 16, 18, 19], by assuming a Markovian arrival process. While one earlier contribution also considers this [11], two key differences make this contribution a better fit for actual buffer optimization: (i) the set of fiber delay lines is assumed to be finite, without restricting the lengths of the fibers, and (ii) the current contribution centers its analysis on the waiting times, rather than on the scheduling horizon (as is done in [11]). Since the description in terms of waiting times spectacularly lowers numerical complexity (as opposed to the complexity of [10, 11]), the model proposed in this paper provides an unmatched tool for optimization, allowing to quantify the impact of correlation in the arrival process on the performance fast and in an exact manner.

The remainder of this paper is organized as follows. In Section 2, we set out the assumptions on the FDL buffer setting and traffic parameters in detail. Section 3 then presents the performance analysis. In Section 4, an efficient numerical recipe is highlighted, allowing to calculate results very fast. Several numerical examples illustrate our approach in Section 5, where the specific impact of correlation in

the arrival process on loss performance is foregrounded. Conclusions are drawn is Section 6, while the mathematical details of Section 4 are included in Appendix.

2. **Performance model.** We consider an optical FDL buffer, operating synchronously. Hence, time is divided into fixed length intervals or slots and all burst arrivals are synchronized with respect to the slot boundaries. In the remainder, we retain the OBS terminology, and a "burst" refers to an inseparable transmission unit in the optical network. The size or transmission times of bursts as well as the delays in the fiber delay lines are expressed as integer multiples of the slot length, which implies that burst departures are synchronized with respect to slot boundaries as well. Hence, all time related quantities are expressed in multiples of the slot length.

Within an optical network, the buffer is located at the output of a backbone switch, and is dedicated to a single outgoing wavelength. Since there is only one wavelength, outgoing burst transmissions cannot overlap. Possible contention is resolved by sending one of the contending bursts through a fiber delay line. Buffer control exercises a first-come-first-served scheduling discipline. If a burst cannot be transmitted instantaneously, it is routed to the shortest delay line such that there is no overlap with the previous burst. However, since the requested delay may not be present in the set of delays, in general, a burst is delayed for somewhat longer than strictly needed, because it has to pass through an entire delay line. This results in"voids" on the outgoing wavelength, that is, periods during which the outgoing wavelength remains unused, despite the fact that bursts are still present in the buffer. Notice that the first-come-first-served scheduling discipline is not the only possible discipline. It is possible that an arriving burst fits into one of the voids that was created upon arrival of a preceding burst. Such a void-filling policy is complicated to analyze and costly to implement (in terms of control logic), does not retain the order of the bursts, and is not considered here.

The buffer consists of a set of N FDLs and can directly forward bursts as well, such that it can assign $N+1$ different delays. Often, the length of the delays is chosen equidistant, with the lengths equal to multiples of the so-called granularity D, resulting in line lengths $0, 1 \times D, 2 \times D \ldots N \times D$. Often (but not always, see [10]), such equidistant setting is optimal in terms of performance; however, the model presented here is valid for arbitrary line lengths. Let $\omega_0 = 0 < \omega_1 < \ldots < \omega_N$ denote the involved delays (corresponding to line lengths), expressed in multiples of the slot length, but further completely arbitrary. As the set of fiber delay lines is intended to resolve contention on a single wavelength, it is necessary that contending bursts undergo different delays. Therefore, a useful FDL set never contains the same length twice. Bursts that need to undergo delays smaller or equal to ω_N can be accommodated; burst that require larger delays cannot be accommodated and are either discarded or sent to another contention resolution interface (for instance, another wavelength), depending on the considered implementation. For ease of notation, we introduce the following operator. Let $\Omega = \{\omega_0, \ldots, \omega_N\}$ denote the set of possible delays, the generalized ceiling operator $\lceil \cdot \rceil_\Omega$ is then defined as follows,

$$\lceil x \rceil_\Omega = \inf\{y \in \Omega, y \geq x\}, \tag{1}$$

for $x \leq \omega_N$.

The burst arrival process is modeled as a discrete-time Markovian arrival process (D-MAP). Numbering consecutive slots by an index s (with s an integer number), let $\hat{Q}_s$ denote the state of the modulating Markov chain during slot s. The consecutive $\hat{Q}_s$ take on values in the finite state space $\mathcal{Q} = \{1, 2, \ldots, M\}$. Furthermore, let T_s

denote the number of bursts arriving in slot s, $T_s \in \{0,1\}$, with bursts arriving upon the slot boundary with which slot s commences. Then, the D-MAP is completely characterized by the $M \times M$ matrices $\mathbf{A}_0$ and $\mathbf{A}_1$ that govern the state transitions from slot s to the next when there are no arrivals and when there is an arrival in a slot, respectively. In other words, the ijth element of $\mathbf{A}_n$ ($n \in \{0,1\}$) equals

$$a_{ij}(n) = \Pr[T_{s+1} = n, \hat{Q}_{s+1} = j | \hat{Q}_s = i]\,. \tag{2}$$

For further use, let $\mathbf{A} = \mathbf{A}_0 + \mathbf{A}_1$ denote the transition matrix of the modulating Markov chain. Note that $\mathbf{A}$ is a stochastic matrix (for each row, the row sum is 1), whereas $\mathbf{A}_0$ and $\mathbf{A}_1$ are substochastic matrices (for one or more rows, the row sum is smaller than one). The latter implies that we exclude the trivial cases $\mathbf{A} = \mathbf{A}_0$ (no arrivals) and $\mathbf{A} = \mathbf{A}_1$ (one arrival each slot).

Finally, the sizes of the consecutive bursts (in multiples of the slot length) are assumed to constitute a sequence of independent and identically distributed (iid) positive random variables. Let $b(l)$, $l \in \mathbb{N}_0$, denote their common probability mass function.

3. Performance analysis.

With the modeling assumptions and the notation established, we now introduce the Markovian system description and construct the corresponding transition matrix. The system state space is two-dimensional with range $\Omega \times \mathcal{Q}$; the transition matrix is thus four-dimensional and has a two-dimensional block representation. The steady-state solution of this chain then results in expressions for various interesting performance measures.

3.1. System equations.

To construct the system equations, we number bursts in the order of their arrival, and choose to number only those bursts that can be accommodated. With this assumption, we consider an arbitrary (accommodated) burst k, and define its waiting time W_k as the time between the slot boundary upon which the burst arrives, say slot s, and the slot boundary upon which its transmission commences, slot $s + W_k$. Since the waiting time is realized by means of the FDLs, $W_k \in \Omega$. Moreover, let B_k and A_k denote the burst size of this burst and the inter-arrival time between burst k and the next. Note that the next burst is not necessarily burst $k+1$, as all bursts that cannot be accommodated remain without index. To characterize this, let $\tilde{A}_{k,j}$ denote the inter-arrival time between burst k and the jth burst arriving at the buffer after burst k. In particular, $A_k = \tilde{A}_{k,1}$. Finally, let Q_k denote the state of the modulating Markov chain during the slot after the kth (accommodated) arrival.

We now construct a Lindley-type recursion for the waiting times of the bursts in the optical queue; we modify the Lindley recursion to account for the particularities of optical buffering. To construct the system equations, a set of two, we consider an (accommodated) burst k. The next burst arrives A_k slots later, and finds the system busy with burst k (and all earlier bursts) for a time $W_k + B_k - A_k$. If this busy time exceeds the longest realizable delay, $W_k + B_k - A_k > \omega_N$, then this next arriving burst cannot be accommodated, and the system is unavailable to all bursts arriving during the next $W_k + B_k - A_k - \omega_N - 1$ slots following that first slot of unavailability (amounting to $W_k + B_k - A_k - \omega_N$ slots of unavailability). In the opposite case, $W_k + B_k - A_k \leq \omega_N$, no unavailability comes about, and the burst following burst k can be accommodated, and is numbered $k+1$. More generally, after the arrival of burst k, the system either experiences a lossless transition to the arrival of burst $k+1$ (the burst following burst k can be accommodated, and is

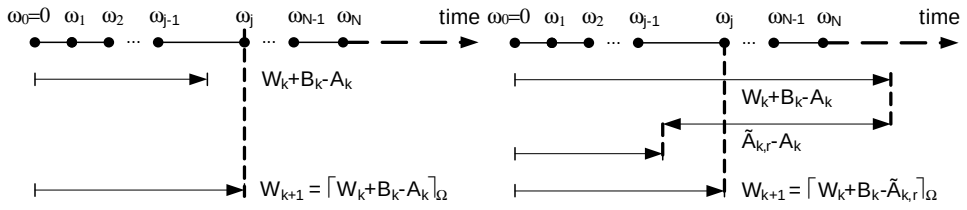

(a) If $Y_k = 0$, W_{k+1} is given by (4). (b) If $Y_k > 0$, W_{k+1} is given by (5).

Figure 1: Depending on the value of Y_k, given by (3), a different system equation applies. This is illustrated for general FDL set $\Omega = \{\omega_0, \ldots, \omega_N\}$ with $\omega_0 = 0$ and general ω_j, $j = 1 \ldots N$.

numbered burst $k+1$), or it experiences a transition with loss (the burst following burst k is lost, and a later-arriving burst is accepted and numbered burst $k+1$). The difference between both can be made by means of the unavailable period Y_k,

$$Y_k = (W_k + B_k - A_k - \omega_N)^+, \tag{3}$$

where $(x)^+$ denotes $\max(0,x)$. The set of system equations now applies to two mutually exclusive events, illustrated in Fig. 1(A) and Fig. 1(B).

· *If* $Y_k = 0$, then the system remains available uninterruptedly, and the burst following burst k can be accommodated regardless of the inter-arrival time between them, and is labeled burst $k+1$. This is illustrated in Fig. 1(A). This corresponds to a burst arriving A_k time slots after the kth burst, which can be accepted, and is numbered $k+1$. The waiting time evolves according to the following (and first) system equation,

$$W_{k+1} = \lceil W_k + B_k - A_k \rceil_\Omega \ . \tag{4}$$

In other words, the fact that $Y_k = 0$ implies that $W_k + B_k - A_k \leq \omega_N$, or, equivalently, that the delay needed in order not to collide with the previously accommodated burst (delay $W_k + B_k - A_k$) is lower than the length of the longest line (length ω_N). As such, a sufficiently long delay line (index j, see Fig. 1(A), $\omega_{j-1} < W_k + B_k - A_k \leq \omega_j$) can always be found and is available.

· *If* $Y_k > 0$, the burst arriving just after the kth cannot be accepted, and it takes an additional time (equal to $\tilde{A}_{k,r} - A_k$, see next) until burst $k+1$ is accepted. This is illustrated in Fig. 1(B). The waiting time evolves according to the following (and second) system equation,

$$W_{k+1} = \left\lceil W_k + B_k - \tilde{A}_{k,r} \right\rceil_\Omega \ . \tag{5}$$

Here, r is defined as

$$r = \inf_j \{\tilde{A}_{k,j}; W_k + B_k - \tilde{A}_{k,j} \leq \omega_N, j \in \mathbb{N}_0\}\,, \tag{6}$$

and is necessarily larger than one, $r > 1$, since at least one burst (associated with $A_{k,1}$) was lost during the transition. In general, $r-1$ bursts arrive during the unavailability period, which lasts for Y_k slots. Burst $k+1$ is the first burst that arrives after the system turns available again, and can again be accommodated.

With the system equations and the modeling assumptions at hand, it is easy to verify that the sequence (W_k, Q_k) constitutes a Markov chain with state space

$\Omega \times \mathcal{Q}$. In the following, we first translate the system equations into expressions for the transition matrix probabilities of the Markov chain. A second step derives steady-state probabilities from this, which lead to the main performance measures in a third step. Finally, it is also highlighted how the scheduling horizon can be expressed in terms of the obtained results. Note that the second step is rather straightforward. Standard algebraic techniques can be applied, since the number of states $(N+1) \times M$ is limited: the number of available fiber delay lines is kept low in practice in order to keep the footprint acceptable (say, no more than $N = 10$), and a modest number of states for the the arriving traffic suffices to model correlation (say, less than 100). As such, the main challenge in the following consists in determining the transition matrix, and the analytic derivation of the performance measures from the steady-state probabilities.

3.2. **Transition matrix.** Consider the system state transition from the acceptance of burst k (state (ω_i, l)) to burst $k+1$ (state (ω_j, m)), and let $\theta(j, m|i, l)$ denote the involved transition probability,

$$\theta(j, m|i, l) = \Pr[W_{k+1} = \omega_j, Q_{k+1} = m | W_k = \omega_i, Q_k = l], \tag{7}$$

for $i, j \in \{0, 1, 2, \ldots, N\}$ and $l, m \in \{1, 2, \ldots, M\}$. Moreover, let $\Theta(j|i)$ denote the $M \times M$ matrix whose lmth entry is $\theta(j, m|i, l)$. Hence, $\Theta(j|i)$ governs the state transitions of the modulating Markov chain on (effective) arrival epochs when the waiting time goes from ω_i to ω_j.

To obtain expressions for the $\theta(j, m|i, l)$, we again employ the unavailable period Y_k (3) in a similar way as we did for the specification of the system equations (4) and (5): if $Y_k = 0$, the next burst can be accommodated; if $Y_k > 0$, at least one burst (and possibly more) is lost during Y_k slots in total. Let $\theta_+(j, m|i, l)$, $\theta_-(j, m|i, l)$ denote the corresponding transition probabilities ("+" for lossless, "−" for loss),

$$\theta_+(j, m|i, l) = \Pr[W_{k+1} = \omega_j, Q_{k+1} = m, Y_k = 0 | W_k = \omega_i, Q_k = l], \tag{8}$$

$$\theta_-(j, m|i, l) = \Pr[W_{k+1} = \omega_j, Q_{k+1} = m, Y_k > 0 | W_k = \omega_i, Q_k = l]. \tag{9}$$

Further, let $\Theta_+(j|i)$ and $\Theta_-(j|i)$ denote the corresponding transition matrices. These matrices obviously relate as follows,

$$\Theta(j|i) = \Theta_+(j|i) + \Theta_-(j|i), \tag{10}$$

and are subsequently determined, according to the value of Y_k.

· *If* $Y_k = 0$, the next burst is accommodated and labeled $k+1$. Its waiting time W_{k+1} equals ω_j if $W_k + B_k - A_k \in (\omega_{j-1}, \omega_j]$. This is illustrated in Fig. 1(A). Following the acceptance of burst k at the start of slot s, burst $k+1$ follows $U_k = B_k - A_k$ slots later, with no arrivals in-between. If $U_k = n \leq 0$, the transition is characterized by $b(l)\mathbf{A}_0^{-n+l-1}\mathbf{A}_1$, with $l \in \mathbb{N}_0$. If $U_k = n > 0$, the transition is characterized by $b(l+n)\mathbf{A}_0^{l-1}\mathbf{A}_1$, with $l \in \mathbb{N}_0$. However, since a transition from ω_i to ω_j is possible with any $U_k = n \in [\omega_{j-1} - \omega_i + 1, \omega_j - \omega_i]$, several values of $W_k + B_k - A_k$ lead to the same waiting time. As such, the outcome is always as illustrated in Fig. 1(A): the smallest delay ω_j which is not smaller than $W_k + B_k - A_k$ is assigned as delay W_{k+1} to burst $k+1$. The corresponding expressions are as follows.

$$\Theta_+(j|i) = \sum_{n=\omega_{j-1}-\omega_i+1}^{\omega_j-\omega_i} \sum_{l=1}^{\infty} b(l + (n)^+)\mathbf{A}_0^{(-n)^+ + l - 1}\mathbf{A}_1, \tag{11}$$

for $i, j \in \{0, 1, \ldots, N\}$. Here, for ease of notation, let $\omega_{-1} \doteq -\infty$ such that the former expression is indeed valid for $j = 0$.

· *If* $Y_k > 0$, the burst following burst k is lost for sure, as $U_k = B_k - A_k = n$ exceeds $\omega_N - \omega_i$; this is characterized by $b(n+\omega_N-\omega_i)\sum_{l=1}^{n-1} \mathbf{A}_0^{l-1}\mathbf{A}_1$, with $n > 1$. This excess is also illustrated on Fig. 1(B), where $W_k + B_k - A_k$ indeed exceeds ω_N. Arriving bursts are discarded during the unavailability period of Y_k slots, with each slot transition characterized by $\mathbf{A}$. As soon as the buffer becomes available again (after Y_k slots), it takes another $m-1$ slots for the next burst to arrive, with the transition characterized by $\mathbf{A}_0^{m-1}\mathbf{A}_1$. Again, a transition to ω_j can be obtained for several subsequent slots, as long as $m \in [\omega_N - \omega_j + 1, \omega_N - \omega_{j-1}]$. As a result, the exact time between burst k and burst $k+1$ is a non-trivial function of the inter-arrival times and a side constraint, as reflected in (6). This is also illustrated in Fig. 1(B), where $\tilde{A}_{k,r} - A_k$ is the time between the arrival of the first burst that was dropped, and the arrival of burst $k+1$. Summarizing, we find,

$$\Theta_-(j|i) = \left(\sum_{n=2}^{\infty} b(n+\omega_N-\omega_i)\sum_{l=1}^{n-1}\mathbf{A}_0^{l-1}\mathbf{A}_1\mathbf{A}^{n-l-1}\right)\sum_{m=\omega_N-\omega_{j-1}}^{\omega_N-\omega_j+1}\mathbf{A}_0^{m-1}\mathbf{A}_1\,. \quad (12)$$

The combination of (11) and (12) suffices to quantify all possible transitions of the two-dimensional Markov chain describing the system's behavior.

Let $\pi_{ij} = \lim_{k\to\infty}\Pr[W_k = i, Q_k = j]$ denote the steady-state probability of the Markov chain (W_k, Q_k), let π_i denote the row vector with elements π_{ij} $(j \in \mathcal{Q})$ and let π denote the row block vector with elements π_i $(i \in \Omega)$. Finally, let Θ denote the $M(N+1)\times M(N+1)$ block matrix whose ijth block is given by $\Theta(j|i)$. The steady-state vector π is then the normalized Perron-Frobenius eigenvector of Θ. That is, the vector π is the unique solution of,

$$\pi = \pi\Theta\,, \quad < \pi, \mathbf{1} >= 1 \quad (13)$$

where $< \mathbf{x}, \mathbf{y} >$ denotes the dot product, and $\mathbf{1}$ is a vector of ones. As already mentioned, the number of Markov states is typically limited, and therefore, well-known standard algebraic techniques can be applied to obtain π.

3.3. **Performance measures.** Given the steady-state vector π, various performance measures are easily found. Obviously, the probability mass function of the delay of an arbitrary burst k is given by,

$$w(x) = \Pr[W_k = x] = \begin{cases} < \pi_i, \mathbf{1} > & \text{for } x = \omega_i, \\ 0 & \text{otherwise.} \end{cases} \quad (14)$$

Hence, the mean and variance of the burst delay are given by,

$$\mathrm{E}[W_k] = \sum_{x\in\Omega} w(x)x\,, \quad \mathrm{Var}[W_k] = \sum_{x\in\Omega} w(x)(x - \mathrm{E}[W_k])^2\,.$$

In order to find an expression for the burst loss ratio, we first focus on the mean number of bursts $\mathrm{E}[X]$ that arrived during the unavailable period following an arbitrary burst k (and therefore could not be accommodated). A similar argument as the one leading to equation (12), yields the following expression,

$$\mathrm{E}[X] =< \sum_{i\in\Omega} \pi_i\mathbf{G}_i, \mathbf{1} > \,. \quad (15)$$

with,

$$\mathbf{G}_i = \sum_{n=2}^{\infty} b(n+\omega_N-\omega_i) \sum_{l=1}^{n-1} \mathbf{A}^{l-1}\mathbf{A}_1 \,. \tag{16}$$

Since on average there are $\mathrm{E}[X]$ bursts that are rejected for every burst that can be accommodated by the optical buffer, the burst loss ratio is given by,

$$\mathrm{BLR} = \frac{\mathrm{E}[X]}{\mathrm{E}[X]+1} \,. \tag{17}$$

3.4. **Scheduling horizon.** As discussed in Section 1, several earlier performance models [8, 15, 10, 11, 17] center on the scheduling horizon. While the approach focusing on the waiting times is more effective for the single-wavelength buffer case, the scheduling horizon is still of use as a reference point. Not only is it more insightful in the single-wavelength case (as it reveals the origin of voids), it also proves indispensable when a more complex buffer setting is studied. For instance, in the case of multiple outgoing wavelengths, say c, a general exact description of the system's evolution requires to include the scheduling horizon of $c-1$ wavelengths in the Markov state description, completed with the last-assigned waiting time of the remaining wavelength (see also [13]). Therefore, we consider it useful to also include the analytic method allowing to generate scheduling horizon probabilities from the results obtained above.

Again considering an arbitrary accommodated burst k, the scheduling horizon H_k is defined as the earliest time at which all previous bursts will have left the system, as seen upon arrival of burst k. The relation to the burst's waiting time is $W_k = \lceil H_k \rceil_\Omega$, and the fore-mentioned voids are defined as $W_k - H_k$. The probability mass function reflects the structure of (4) and (5), as

$$H_{k+1} = \begin{cases} (W_k + B_k - A_k)^+ & \text{for } Y_k = 0, \\ (W_k + B_k - \tilde{A}_{k,r})^+ & \text{for } Y_k > 0, \end{cases} \tag{18}$$

with r as defined in (6). In view of these expressions, one then shows that the probability mass function of the scheduling horizon is given by,

$$h(l) = \Pr[H_k = l] = < \sum_{i\in\Omega} \pi_i \hat{\Theta}(l|i), \mathbf{1} > \,, \tag{19}$$

for $l = 1, \ldots, \omega_N$, with $\hat{\Theta}(l|i) = \hat{\Theta}_+(l|i) + \hat{\Theta}_-(l|i)$ and with,

$$\hat{\Theta}_+(l|i) = \sum_{n=(l-\omega_i)^++1}^{\omega_N-\omega_i+1} b(n)\mathbf{A}_0^{\omega_i+n-l-1}\mathbf{A}_1 \,, \tag{20}$$

$$\hat{\Theta}_-(l|i) = \sum_{n=\omega_N-\omega_i+2}^{\infty} b(n)\mathbf{A}^{\omega_i+n-\omega_N-1}\mathbf{A}_0^{\omega_N-l}\mathbf{A}_1 \,. \tag{21}$$

Further, note that $h(0) = w(0)$. Also, note that the scheduling horizon is upper-bounded, $H_k < \omega_N$, since it is associated with accommodated bursts, for which a suitable delay was indeed found present within the FDL set. From this point, the mean and variance are easily obtained as

$$\mathrm{E}[H_k] = \sum_{l=1}^{\omega_N} h(l)l \,, \quad \mathrm{Var}[H_k] = \sum_{l=0}^{\omega_N} h(l)(l-\mathrm{E}[H_k])^2 \,.$$

B_m	$N = 10$	$N = 20$	$N = 100$
10	0.4507	1.4667	38.7322
100	0.4752	1.5314	40.6626
1000	0.8439	2.0815	41.8155

Table 1: Time (in seconds) needed to calculate 100 BLR values ($D = 1, 2 \ldots 100$), for various values of the buffer size N and the maximum burst size B_m.

4. **Numerical recipe.** If one applies the formulas in the form in which they are given, calculating the coefficients of the matrix Θ is more time-consuming than calculating the steady-state vector. Moreover, both Θ_+ and Θ_- contain infinite sums, which can either be truncated, or, alternatively, be dealt with by means of the spectral decomposition of $\mathbf{A}$, $\mathbf{A}_0$ and $\mathbf{A}_1$, transforming the infinite sums into finite sums of the probability mass function and the probability generating function of the burst size. However, even then, calculation time poses problems especially with Ω_N, N, M large. Since we are typically interested in BLR values for an entire range of possible FDL sets Ω (typically, BLR curves for 10 to 100 values of the above-mentioned granularity D), it is useful to look for numerical recipes which lower the total calculation time of an entire BLR curve. Therefore, we developed a two-step numerical recipe that decomposes all probabilities in sums and products of coefficients $C_i(l)$, $i = 1, 2 \ldots 9$, $l \in \mathbb{Z}$, which are independent of Ω. As such, when one evaluates the performance of various FDL sets Ω while maintaining the same arrival and burst size characteristics, the coefficients only need to be calculated once for the entire evaluation. The numerical recipe consists in the calculation of the coefficients in the first step, and only combines the coefficients to probabilities in the second step.

For the exact mathematical details, we refer the reader to the Appendix; here, we limit ourselves to a small overview of calculation times in Table 1, with the same parameter settings as in Fig. 2(A) (and `arr2`, see further) except where indicated. For all calculations, we used Matlab R2008b on a standard notebook (Intel Core 2 Duo CPU P9600@2.64GHz, 4.00 GB RAM running 64 bit OS). As can be seen, calculation time quickly grows with the number of FDLs N. This is natural since it determines the number of Markov states, and does not pose problems for the small N used in practice. Although not shown explicitly, augmenting the number of arrival states M has a similar impact; again, this poses no stumble block since a limited number of states suffices to model correlation. A specific merit of the numerical recipe we developed is that calculation time is hardly impacted by the maximum burst size B_m, defined as $\sup_i\{b(i) : b(i) > 0\}$. Since burst sizes in OBS are subject to an upper-bound for technical reasons, we have only examined numerical examples for which such an upper-bound exists. However, the fact that our recipe is insensitive to B_m opens perspectives for the case of an unbounded burst size distribution, for which an accurate approximation can be made by truncating the burst size distribution at some sufficiently high value of B_m.

5. **Numerical examples.** With the formulas at hand, we now apply the numerical recipe to some numerical examples, chosen to investigate the impact of arrival correlation on the performance of the optical buffer. The figures included in this paper depict the burst loss ratio as function of the granularity D. As mentioned earlier,

tag	α	β	γ
arr0	1	0	0
arr1	0.6	0.2	0.85
arr2	0.6	0.2	0.95
arr3	0.6	0.2	0.98

(a) arrivals

	Q	range	E[B]	B_m
deterministic	0	[61]	61	61
uniform	10	[41,61]	51	61
uniform	30	[1,61]	31	61

(b) burst size

Table 2: Parameter settings of the arrival process and of the burst size distribution.

these BLR curves play a paramount role in the optimization of optical buffers, as the choice of the granularity D is fixed during production and its value is critical to the performance of the buffer. Given a certain traffic setting (arrival process, burst size distribution, traffic load), the BLR curves allow to determine optimal values of the traffic load, and also point out the impact of a mismatch between optimal granularity and implemented granularity.

For deterministic burst size distribution (burst sizes fixed to B_m), a rule of thumb is known in case of Bernoulli arrivals [8], and consists in matching the granularity with the burst size value, $D = B_m - 1$. (The term -1 is the result of an offset, characteristic to the discrete-time setting. In a continuous-time setting, the rule of thumb simplifies to $D = B_m$ [15].) Such a choice guarantees minimal loss, but only for traffic loads below a threshold load ρ_{th} of about 0.6 (where the exact value of ρ_{th} depends slightly on the exact value of N and B_m [19]). As will be demonstrated further on, the rule of thumb largely holds when correlation comes about. For general (non-deterministic) burst size however, the optimal granularity is highly dependent on the level of correlation, range of the burst size distribution and the value of the traffic load. We first present the traffic setting assumptions, to then apply these to obtain actual BLR curves.

5.1. **Traffic setting.** For the arrival process, we choose a a tunable process with three states ($M = 3$), associated with high arrival intensity, low arrival intensity and zero arrival intensity (no arrivals), respectively. Correspondingly, the probability of a burst arriving at the beginning of an arbitrary slot is p in state 1, $p/5$ in state 2 and 0 in state 3. Further, the arrival process remains in state 1, 2 and 3 with probability α, β and γ, respectively. State changes are only possible to neighboring states and have equal probability. The resulting process is characterized by periods without activity (no arrivals) (in state 3, average duration $1/\gamma$ slots), alternated by periods of activity with either low activity (state 2, intensity $p/5$, average duration $1/\beta$ slots) or a sequence of warm-up (state 2, intensity $p/5$, average duration $1/\beta$ slots), high activity (state 1, intensity p, average duration $1/\alpha$ slots) and cool-down (state 2, average duration $1/\beta$ slots, intensity $p/5$). Hence, the transition matrices equal $\mathbf{A}_0 = (\mathbf{I} - \mathbf{P})\mathbf{A}$ and $\mathbf{A}_1 = \mathbf{P}\mathbf{A}$ with,

$$\mathbf{A} = \begin{bmatrix} \alpha & 1-\alpha & 0 \\ \frac{1-\beta}{2} & \beta & \frac{1-\beta}{2} \\ 0 & 1-\gamma & \gamma \end{bmatrix}, \quad \mathbf{P} = \begin{bmatrix} p & 0 & 0 \\ 0 & \frac{p}{5} & 0 \\ 0 & 0 & 0 \end{bmatrix}, \tag{22}$$

and whereby $\mathbf{I}$ denotes the identity matrix (with dimension $M \times M$ like $\mathbf{A}$). The parameter settings considered below are displayed in Table 2, and are referred to

by tags `arr0`, `arr1`, `arr2` and `arr3`, sorted in order of increasing correlation. The steady-state probabilities $\pi_A(l)$ of finding the arrival Markov chain in state l at the beginning of an arbitrary slot equal

$$\pi_A = \frac{1}{\bar{\alpha}\bar{\beta} + 2\bar{\alpha}\bar{\gamma} + \bar{\beta}\bar{\gamma}} \left[\bar{\beta}\bar{\gamma}\ ,\ 2\bar{\alpha}\bar{\gamma}\ ,\ \bar{\alpha}\bar{\beta}\right]\ ,$$

where $\bar{x}$ is shorthand for $1 - x$. The average arrival intensity λ follows easily, as

$$\lambda = \pi_A(1)p + \pi_A(2)\frac{p}{5} = p\frac{5\bar{\beta}\bar{\gamma} + 2\bar{\alpha}\bar{\gamma}}{\bar{\alpha}\bar{\beta} + 2\bar{\alpha}\bar{\gamma} + \bar{\beta}\bar{\gamma}}\,.$$

For the burst size distribution, as usual in OBS, the burst sizes are subject to some maximum burst size B_m; we consider a uniform distribution with range parameter Q, and corresponding probability mass function,

$$b(n) = \begin{cases} 1/(2Q+1) & n \in [B_0 - Q, B_0 + Q]\,, \\ 0 & n \notin [B_0 - Q, B_0 + Q]\,. \end{cases}$$

with B_0 defined as $B_0 = B_m - Q$, and $\mathrm{E}[B] = B_0$. As displayed in Table 2, the parameter settings considered below have $B_m = 61$ slots, and differ in the value of Q: $Q = 0$ produces a deterministic distribution, $Q = 10$ slots a uniform distribution with narrow range, and $Q = 30$ slots a uniform distribution with wide range.

The traffic load ρ is defined in the usual way, as $\rho = \lambda \mathrm{E}[B] = \lambda(B_m - Q)$. We further assume that the FDLs are equidistant, $\omega_i = iD$, with D the above-mentioned granularity of the optical buffer.

As said, the arrival process settings are tagged `arr0`, `arr1`, `arr2` and `arr3` in increasing order of correlation. More precisely, `arr0` has the arrival transitions limited to recurrence to state 1, so producing a Bernoulli arrival process, a memoryless process (no correlation) constituting the discrete-time counterpart to the (continuous-time) Poisson process. For `arr1`, `arr2` and `arr3`, the length of the periods without arrivals (average duration $1/\gamma$ slots) is increased, producing more correlation and higher intensity p during activity periods, while maintaining the same overall traffic load ρ (and, corresponding, the same λ). This mechanism is put to use in several numerical examples below.

5.2. **BLR curves.** Figures 2 and 3 illustrate the impact of correlation on buffer performance, for a burst size distribution that is either deterministic, narrow-ranged uniform ($Q = 10$) or wide-ranged uniform ($Q = 30$), respectively. The buffer size is $N = 10$, the traffic load is $\rho = 0.6$, the maximum burst size is $B_m = 61$, and the arrival and burst size characteristics are as given in Table 2. Obvious in all four figures is that arrival correlation has a negative effect on the buffer's loss performance, as could be expected, since this is also the case for classic RAM buffers. Less obvious is the impact of arrival correlation on the (local) performance optima, discussed earlier in the case of uncorrelated arrivals in [8, 19] and corresponding to granularity values $D = (B_m - 1)/n$, with $n = 1, 2, \ldots N$. In case of deterministic burst size distribution, it can be understood from Fig. 2(A) that matching D with $B_m - 1$ is markedly optimal, as the performance gap between this and other possible choices for D (such as $D = (B_m - 1)/2$) grows as correlation increases. More complicated is the situation of uniform burst size distribution. Apparently, for the narrow-ranged uniform distribution ($Q = 10$) of Fig. 2(B), increased correlation leads to a shift in optimal granularity, from (about) $B_m/2$ for `arr0` and `arr1`, to $B_m - 1$ for `arr2` and `arr3`. This trend is also illustrated in Fig. 3(A), where this

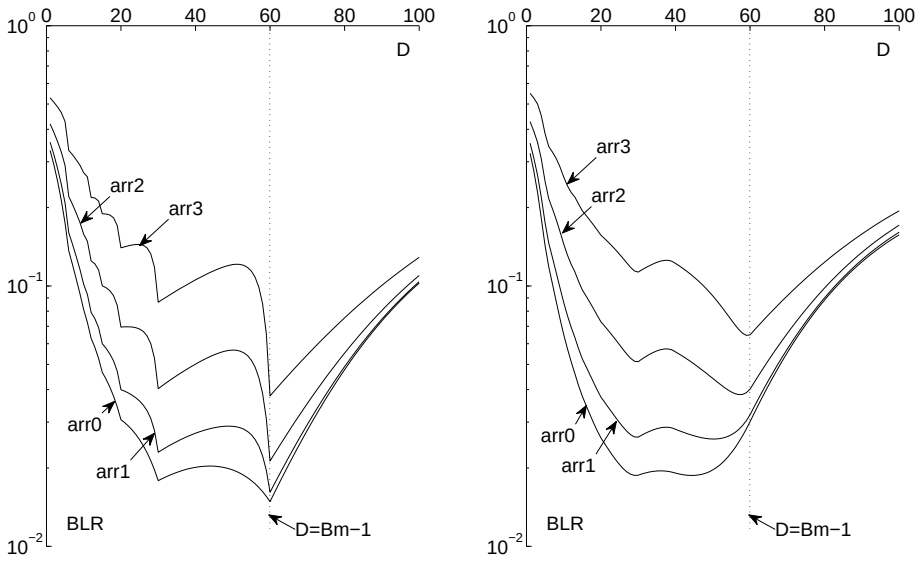

(a) deterministic burst size distribution with $\mathrm{E}[B] = B_m = 61$

(b) uniform burst size distribution with $\mathrm{E}[B] = 51$, $B_m = \mathrm{E}[B] + Q = 61$

Figure 2: Increasing arrival correlation (`arr0` to `arr3`) leads to an increased BLR. However, depending on the burst size distribution, the optimal granularity does not change if burst size is fixed ($D = B_m - 1$, see left pane), while it does change for a uniform distribution, moving to $D = B_m - 1$ (right pane, see also Fig. 3).

is compared to the results for deterministic burst size distribution. For the broad-ranged uniform burst size distribution ($Q = 30$) of Fig. 3(B), increased correlation changes the shape of the curves, but the optimum consistently remains near $D = \mathrm{E}[B] - 1$. As such, in general, the robustness to correlation motivates the choice of long delay lines ($D \approx B_m$) if the variation of burst sizes is small (narrow range), whereas shorter delay lines ($D \approx \mathrm{E}[B]$) are recommendable if the variation of burst size is large (wide range).

While Fig. 2 and 3 consider the interplay between arrival correlation and burst size distribution, Fig. 4 focuses on the impact of buffer size and load, and only considers one case of arrival correlation (`arr2`) and two burst size distributions ($Q = 0$ and $Q = 10$). From Fig. 4(A), we learn that a change in buffer size ($N = 10$ to $N = 20$) does improve performance, but does not impact the shape or optima of the curves. This "invariance" was also observed for uncorrelated arrivals [16] for sufficiently large N (say, $N > 5$) and somewhat simplifies the optimization process, as the optimization is largely insensitive to the exact value of N. Different is the impact of the load ρ, displayed in Fig. 4(B). In both cases of the burst size distribution ($Q = 0$ and $Q = 10$), the optimum $D = B_m - 1$ for $\rho = 0.6$ is also the optimum for $\rho = 0.3$, as can be seen on the figure. Results not shown here confirm that $D = B_m - 1$ is optimal for any load $\rho \in [0, 0.6]$. However, when the load is

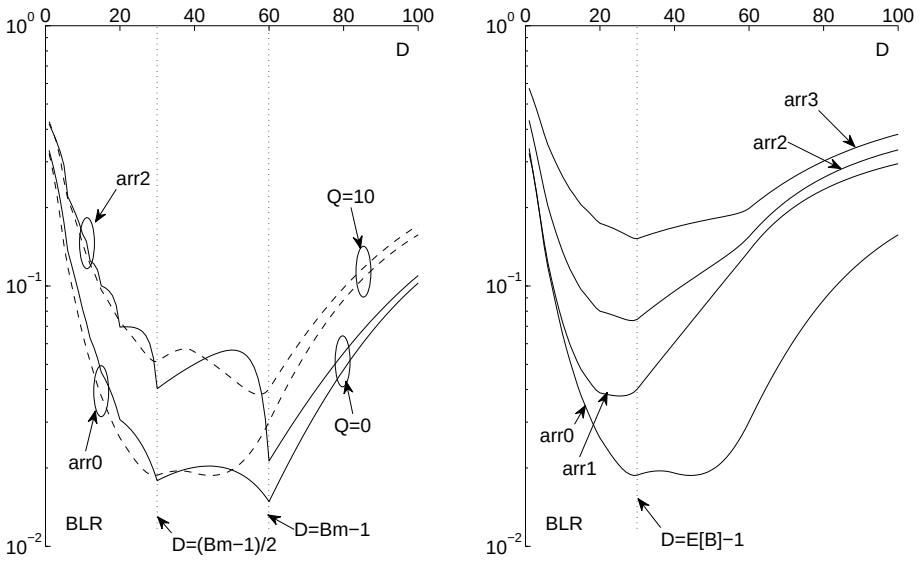

(a) deterministic ($\mathrm{E}[B] = B_m = 61$) and uniform(b) uniform burst size distribution with $\mathrm{E}[B] =$
($Q = 10$, $B_m = 61$) burst size distribution com-31, $B_m = \mathrm{E}[B] + Q = 61$
pared

Figure 3: Comparing the BLR of deterministic and narrow-ranged burst size distribution (left pane), the same trend is observed: increased correlation results in large performance loss for $D = (B_m - 1)/2$, and small performance loss for $D = D_m - 1$. For wide-ranged uniform burst size distribution (right pane), increasing arrival correlation (`arr0` to `arr3`) also alters the shape of the BLR curves, but with optimal D always near to $\mathrm{E}[B]$.

further increased, the optimal granularity shifts to lower values, and this regardless of the burst size distribution. This observation was also made for uncorrelated arrivals [19]; the main difference is that the optimum for large granularity is more robust to load increase in the presence of correlation. As such, again, the presence of arrival correlation motivates the choice of a larger granularity ($D \approx B_m$), and thus relatively longer delay lines.

6. **Conclusions.** In this paper, we presented a Markovian model for a synchronous optical buffer. The model is quite general: a general set of FDLs, correlated arrivals and generally-distributed burst sizes. Exploiting the fact that the buffer can only assign a small number of waiting times, an efficient numerical procedure was developed which calculates various performance measures fast. The presented results include a light-weight algorithm, which has minimal numerical complexity and provides the starting point for a more extensive optimization study on the impact of correlation, that could shed light on the complex interplay between all involved variables. By means of several numerical examples, we illustrated the impact of

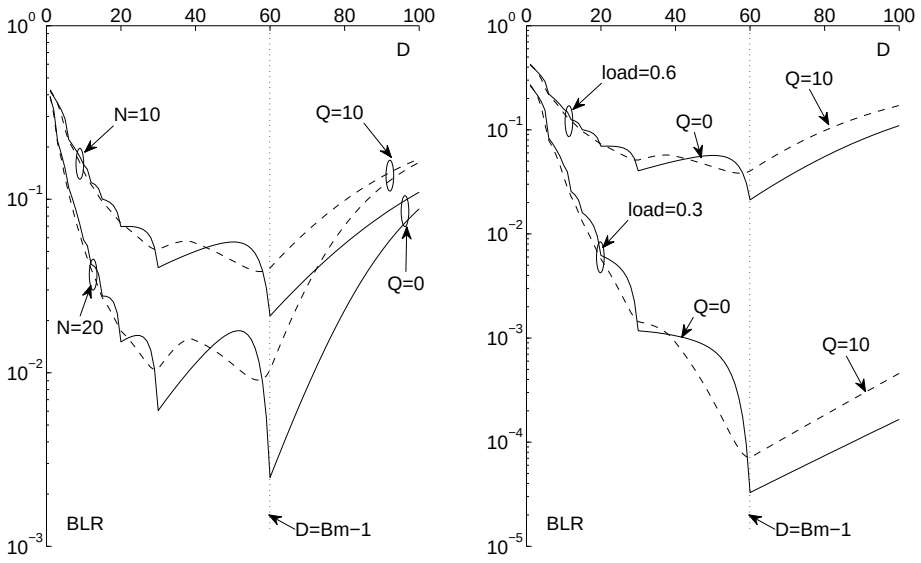

(a) buffer size $N = 10$ vs. $N = 20$

(b) load $\rho = 0.3$ vs. $\rho = 0.6$

Figure 4: Although the overall loss decreases with increasing N, the (local) optimality of special values of D ($D = B_m - 1$, $D = (B_m - 1)/2$) does not change. Further, the shape of the curves hardly changes as N increases (left pane), while it is strongly impacted when the traffic load changes (right pane).

arrival correlation on optical buffer performance. Results show that the presence of arrival correlation motivates the choice of a relatively large granularity, since such a setting has good performance in case of uncorrelated arrivals, and is optimal in case of correlation.

Acknowledgments. The authors wish to thank K. De Turck for his valuable input and insights (matrix-analytic methods!) during the writing of this paper.

Appendix: Numerical recipe mathematics. As mentioned in Section 4, we developed a two-step numerical recipe that decomposes all probabilities in sums and products of coefficients $C_i(l)$, $i = 1, 2 \ldots 9$, $l \in \mathbb{Z}$, which are independent of Ω. As such, when one evaluates the performance of various FDL sets Ω while maintaining the same arrival and burst size characteristics, the coefficients only need to be calculated once for the entire evaluation. The numerical recipe consists in the calculation of the coefficients in the first step, and only combines the coefficients to probabilities in the second step, to obtain the desired matrices $\Theta_+(j|i)$ (11), $\Theta_-(j|i)$ (12) and $\mathbf{G}_i$ (16). Since the involved formulas are somewhat hard to obtain, but not necessarily very insightful, we limit ourselves to stating them, and do not comment on each expression separately.

$$
\begin{array}{lcll}
\mathbf{C}_1(l) & = & \mathbf{A}^l & 1 \le l \le B_m + L - 1 \\
\mathbf{C}_2(l) & = & \sum_{i=1}^{l-1} \mathbf{C}_1(i) = \sum_{i=1}^{l-1} \mathbf{A}^{i-1}\mathbf{A}_1 & 1 \le l \le B_m + L - 1 \\
\mathbf{C}_3(l) & = & \mathbf{A}_0^{l-1}\mathbf{A}_1 & 1 \le l \le B_m + L \\
\mathbf{C}_4(l) & = & \sum_{i=1}^{l} \mathbf{C}_3(i) = \sum_{i=1}^{l} \mathbf{A}_0^{i-1}\mathbf{A}_1 & 0 \le l \le B_m + L \\
\mathbf{C}_5(l) & = & \sum_{i=1}^{l-1} \mathbf{C}_4(i)\mathbf{C}_1(l-i-1) & 1 \le l \le B_m + L \\
 & = & \sum_{i=1}^{l-1} \mathbf{A}_0^{i-1}\mathbf{A}_1\mathbf{A}^{l-i-1} & \\
\mathbf{C}_6(l) & = & \sum_{i=1}^{B_m-(l)^+} b(i+(l)^+)\mathbf{C}_3(i+(-l)^+) & -L \le l \le max(B_m, L) \\
 & = & \sum_{i=1}^{B_m-(l)^+} b(i+(l)^+)\mathbf{A}_0^{(-l)^+ + i - 1}\mathbf{A}_1 & \\
\mathbf{C}_7(l) & = & \sum_{i=-\infty}^{l} \mathbf{C}_6(i) & -L \le l \le +L \\
 & = & (\mathbf{I} - \mathbf{A}_0)^{-1}\mathbf{A}_1 - \sum_{i=l+1}^{B_m} \mathbf{C}_6(l) & \\
\mathbf{C}_8(m) & = & \sum_{i=2}^{B_m-m} b(i+m)\mathbf{C}_5(i) & 0 \le m \le L \\
 & = & \sum_{i=2}^{B_m-m} b(i+m) \sum_{l=1}^{i-1} \mathbf{A}_0^{l-1}\mathbf{A}_1\mathbf{A}^{i-l-1} & \\
\mathbf{C}_9(m) & = & \sum_{i=2}^{B_m-m} b(i+m)\mathbf{C}_2(i) & 0 \le m \le L \\
 & = & \sum_{i=2}^{B_m-m} b(i+m) \sum_{l=1}^{i-1} \mathbf{A}^{l-1}\mathbf{A}_1 &
\end{array}
$$

Table 3: Definition of the coefficients $\mathbf{C}_i(l)$.

$$
\begin{array}{lcll}
\mathbf{C}_5(l) & = & \mathbf{C}_5(l-1)\mathbf{A} + \mathbf{C}_3(l-1) & 1 \le l \le B_m + L \\
\mathbf{C}_6(0) & = & \sum_{i=1}^{B_m} b(i)\mathbf{C}_3(i) & \\
\mathbf{C}_6(max(B_m, L)) & = & \mathbf{0} & \\
\mathbf{C}_6(l-1) & = & \mathbf{A}_0\mathbf{C}_6(l) & -L < l \le 0 \\
 & = & \mathbf{A}_0\mathbf{C}_6(l) + b(l)\mathbf{A}_1 & 1 < l \le max(B_m, L) \\
\mathbf{C}_7(L) & = & (\mathbf{I} - \mathbf{A}_0)^{-1}\mathbf{A}_1 & \\
 & & - \sum_{i=L+1}^{B_m} \mathbf{C}_6(l) & \\
\mathbf{C}_7(l-1) & = & \mathbf{C}_7(l) - \mathbf{C}_6(l) & -L < l \le +L \\
\mathbf{C}_8(L) & = & \sum_{i=2}^{B_m-L} b(i+L)\mathbf{C}_5(i) & \\
\mathbf{C}_8(m-1) & = & b(m+1)\mathbf{A}_1 & 0 < m \le L \\
 & & + \mathbf{C}_8(m)\mathbf{A} + \mathbf{A}_0\mathbf{C}_6(m+1) & \\
\mathbf{C}_9(L) & = & \sum_{i=2}^{B_m-L} b(i+L)\mathbf{C}_2(i) & \\
\mathbf{C}_9(m-1) & = & b(m+1)\mathbf{C}_2(2) + \mathbf{A}\mathbf{C}_9(m) & 0 < m \le L \\
 & & + \left(\sum_{i=m+2}^{B_m} b(i)\right)\mathbf{A}_1 &
\end{array}
$$

Table 4: Recursive expressions for the coefficients $\mathbf{C}_i(l)$.

Step 1: calculating the coefficients. To proceed, we introduce some upper bound L, which equals (but can also be larger than) the maximum delay line value involved in the optimization process. Further, we assume some value B_m. For upper-bounded burst size distribution, this is $\sup_i\{b(i) : b(i) > 0\}$. For unbounded burst size distribution $b_u(i)$, $i \in \mathbb{N}$, $\sum_{i=1}^{\infty} b_u(i)$, one could assume an approximating burst size distribution $b(i) = cb_u(i)$, $i \in \{1, 2 \dots B_m\}$. Here, B_m is a truncation parameter, and c is normalization constant (chosen such that $\sum_{i=1}^{B_m} b(i) = 1$, that is,

$c = (\sum_{i=1}^{B_m} b(i))^{-1}$). Although this is not investigated explicitly in this paper, as discussed in Section 4, it is natural that high accuracy can be obtained by choosing B_m sufficiently large, which is also confirmed by results not included here. In Table 3, the coefficients $\mathbf{C}_i(l)$ are defined one by one. For optimal calculation of these coefficients, it is best to follow a recursive approach. Omitting the cases for which recursive calculation is trivial, we obtain the expressions displayed in Table 4. Note that all are independent of the specific set Ω.

Step 2: obtaining the probabilities. From this point, obtaining the desired matrices $\Theta_+(j|i)$ (11), $\Theta_-(j|i)$ (12) and $\mathbf{G}_i$ (16) is straightforward. It suffices to plug the values of Ω into the following expressions,

$$\Theta_+(j|i) = \mathbf{C}_7(\omega_j - \omega_i) - \mathbf{C}_7(\omega_{j-1} - \omega_i)\,,$$
$$\Theta_-(j|i) = \mathbf{C}_8(\omega_N - \omega_i)\,[\mathbf{C}_4(\omega_N - \omega_{j-1}) - \mathbf{C}_4(\omega_N - \omega_j)]\,,$$
$$G_i = \mathbf{C}_9(\omega_N - \omega_i)\,.$$

Here, note that

$$\mathbf{C}_4(+\infty) = \mathbf{C}_7(+\infty) = (\mathbf{I} - \mathbf{A}_0)^{-1}\mathbf{A}_1.$$

REFERENCES

[1] R. Almeida, J. Pelegrini and H. Waldman, *A generic-traffic optical buffer modeling for asynchronous optical switching networks*, IEEE Communications Letters, **9** (2005), 175–177.

[2] F. Callegati, *On the design of optical buffers for variable length packet traffic*, Proceedings of the Ninth International Conference on Computer Communication and Networks, Las Vegas, (2000), 448–452.

[3] F. Callegati, *Optical buffers for variable length packets*, IEEE Communications Letters, **4** (2000) 292–294.

[4] F. Callegati, *Approximate modeling of optical buffers for variable length packets*, Photonic Network Communications, **3** (2001), 383–390.

[5] Y. Chen, C. Qiao and X. Yu, *Optical burst switching: A new area in optical networking research*, IEEE Network, **18** (2004), 16–23.

[6] T. El-Bawab and J. Shin, *Optical packet switching in core networks: Between vision and reality*, IEEE Communications Magazine, **40** (2002), 60–65.

[7] H. E. Kankaya and N. Akar, *Exact analysis of single-wavelength optical buffers with feedback Markov fluid queues*, Journal of Optical Communications and Networking, **1** (2009), 530–542.

[8] K. Laevens and H. Bruneel, "Analysis of a Single-Wavelength Optical Buffer," Proceedings of IEEE Infocom, San Francisco, 2003.

[9] L. Lakatos, *On a simple continuous cyclic-waiting problem*, Festschrift for the 50th birthday of Karl-Heinz Indlekofer, Annales Univ. Sci. Budapest., Sect. Comp., **14** (1994), 105–113.

[10] J. Lambert, B. Van Houdt and C. Blondia, *Single-wavelength optical buffers: non-equidistant structures and preventive drop mechanisms*, Proceedings of NAEC, Riva del Garda (2005), 545—555.

[11] J. Lambert, B. Van Houdt and C. Blondia, *Queues with correlated service and inter-arrival times and their application to optical buffers*, Stochastic Models, **22** (2006), 233–251.

[12] J. Lambert, W. Rogiest, B. Van Houdt, D. Fiems, C. Blondia and H. Bruneel, *A Hessenberg Markov chain for fast fibre delay line length optimization*, Proceedings of ASMTA 2008, Lecture Notes in Computer Science, **5005** (2008), 101–113.

[13] J. F. Pérez and B. Van Houdt, *Wavelength allocation in an optical switch with a fiber delay line buffer and limited-range wavelength conversion*, Telecommunication Systems, **41** (2009), 37–49.

[14] C. Qiao and M. Yoo, *Optical burst switching (OBS) - a new paradigm for an optical internet*, Journal of High Speed Networks, **8** (1999), 69–84.

[15] W. Rogiest, K. Laevens, D. Fiems and H. Bruneel, *A performance model for an asynchronous optical buffer*, Performance Evaluation, **62** (2005), 313–330.

[16] W. Rogiest, D. Fiems, K. Laevens and H. Bruneel, *Tracing an optical buffer's performance: An effective approach*, Proceedings of Net-COOP, Avignon. Lecture Notes in Computer Science, **4465** (2007), 185–194.

[17] W. Rogiest, K. Laevens, J. Walraevens and H. Bruneel, *Analyzing a degenerate buffer with general inter-arrival and service times in discrete time*, Queueing Systems, **56** (2007), 203–212.

[18] W. Rogiest, D. Fiems, K. Laevens and H. Bruneel, *A light-weight performance model for optical buffers*, International Journal of Communication Networks and Distributed Systems (IJCNDS), **1** (2008), 282–295.

[19] W. Rogiest, J. Lambert, D. Fiems, B. Van Houdt, H. Bruneel and C. Blondia, *A unified model for synchronous and asynchronous FDL buffers allowing closed-form solution*, Performance Evaluation, **66** (2009), 343–355.

Received September 2009; 1st revision January 2010; 2nd revision April 2010.

E-mail address: wrogiest@telin.UGent.be
E-mail address: Dieter.Fiems@UGent.be
E-mail address: kl@telin.UGent.be
E-mail address: hb@telin.UGent.be